Geometry of the Energy Momentum Mapping of the Spherical Pendulum

by R. Cushman

0. Introduction

Reconsideration of the spherical pendulum of classical mechanics with modern mathematical techniques has revealed the occurrence of monodromy in the way level sets of the energy momentum mapping fit together.

This phenomenon has been observed in Duistermaat [1], where the proof of its existence uses rather heavy results. Monodromy is a phenomenon which was not classically investigated because it deals with how certain families of energy momentum level sets fit together and hence can not be observed by looking at motions of a fixed energy and angular momentum. The main point of this article is to give a visual geometric argument which computes the monodromy in the spherical pendulum.

The first part of this article treats the spherical pendulum of classical mechanics from the point of view of Smale's program [4]. Specifically, we study the energy momentum mapping of the spherical pendulum which assigns to every point in phase space (the tangent bundle of the two sphere) the pair of real numbers given by the values of the total energy and angular momentum at that point. Because energy and angular momentum are conserved quantities [2,5], the spherical pendulum is completely integrable. Moreover the fibers of the energy momentum mapping are the sets of all positions and velocities with a given energy and angular momentum.

A well-known theorem of Arnold [1] seems to say that all the fibers, if connected, compact and smooth, are two dimensional tori. But this is only true if the derivative of the energy momentum mapping is surjective. Arnold's theorem does not apply to those motions of the spherical pendulum which are circles parallel to the equator of the two sphere. Thus we give here a careful geometric treatment of the topology of the fibers of the energy momentum mapping of the spherical pendulum. But this is not a complete qualitative description of the spherical pendulum, because the energy momentum mapping has monodromy. The monodromy will be treated in the second part of this article. Proofs are by pictures!

1. Smale's program

a. The energy momentum mapping.

We start with the construction of the energy momentum mapping of the spherical pendulum. For the basic physics of the spherical pendulum, see [5] p. 334 or [6]. Recall that the spherical pendulum is a particle of unit mass

moving on a two sphere S^2 of unit radius under a constant vertical gravitational force of unit strength. Therefore phase space is the tangent bundle TS^2 of S^2, that is,

$$TS^2 = \left\{ (x,v)=(x_1,x_2,x_3,v_1,v_2,v_3)\in\mathbb{R}^3\times\mathbb{R}^3 \;\middle|\; \begin{matrix} x_1^2+x_2^2+x_3^2=1 \\ x_1v_1+x_2v_2+x_3v_3=0 \end{matrix} \right\}$$

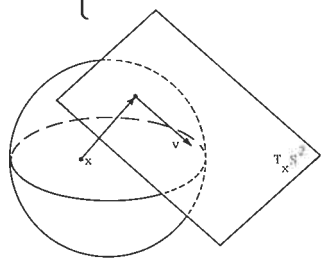

Figure 1.
A tangent plane T_xS^2 to the 2-sphere S^2 at the point x.

with projection $\pi: TS^2 \to S^2 : (x,v) \mapsto x$. Pictorially elements of the tangent space T_xS^2 to S^2 at x are represented by arrows with tail at x and perpendicular to x (Figure 1). TS^2 is the disjoint union of all tangent spaces. The Hamiltonian function of the spherical pendulum is the sum of the kinetic and potential energy of the particle and is the function

$$H:\ TS^2 \to \mathbb{R} : (x,v) \ \mapsto\ \tfrac{1}{2}\|v\|^2 + x_3 \ =\ \tfrac{1}{2}(v_1^2+v_2^2+v_3^2)+x_3.$$

Since a rotation of S^2 about the x_3-axis is a symmetry of the spherical pendulum, there is a corresponding conserved quantity (=integral) called the angular momentum, which is the function

$$L:\ TS^2 \to\ \mathbb{R} : (x,v)\ \mapsto\ x_2v_1 - x_1v_2.$$

Combining the energy and the angular momentum gives the energy momentum mapping

$$\mathcal{EM}:\ TS^2 \to\ \mathbb{R}^2 : (x,v)\ \mapsto\ (H(x,v),L(x,v)).$$

b. Critical points and critical values

To analyze the energy momentum mapping, the first order of business is to find its critical points, that is, points where its derivative $D\mathcal{EM}$ is not surjective. The rank of $D\mathcal{EM}$ is zero at the critical points of H (= critical points of L). These are precisely the equilibrium points of the spherical pendulum where the particle does not move, that is $(n,0)$, $(s,0)\in TS^2$ where n (respectively s) are the north (respectively south) pole of S^2. The corresponding critical values of $\mathcal{EM}$ are (1,0) and (−1,0).

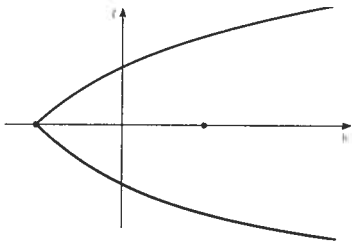

Figure 2.
Image of energy momentum mapping of spherical pendulum.
Darkened curve is energy momentum values of relative equilibria.
Large dots are energy momentum values of equilibria.

The rank of $D\mathcal{EM}$ is one when the derivatives of H and L are linearly dependent. This dependency occurs only on those orbits of the Hamiltonian system which are also orbits of the axial symmetry. Such orbits are called relative equilibria. In the spherical pendulum the relative equilibria are circles on S^2 which lie in a horizontal plane cutting the southern hemisphere. Calculations show that for a given noncritical value h of H, the angular momentum L attains its maximum and minimum values on the relative equilibria. Furthermore, calculations show that the darkened curves in Figure 2 are the critical values of $\mathcal{EM}$ corresponding to the relative equilibria. The image of $\mathcal{EM}$ is the region in Figure 2 bounded by the darkened curves.

c. Regular fibers

The set of regular values $\mathcal{R}$ of the energy momentum mapping consists of those points in the image which are not critical values. If $r=(h,l)\in\mathcal{R}$, then $\mathcal{T}_r=\mathcal{EM}^{-1}(r)$ is a regular fiber. Our next task is to determine the topological type of the regular fibers. Because r is a regular value of $\mathcal{EM}$, Arnold's theorem [1] implies that each connected component of $\mathcal{T}_r$ is a smooth two dimensional torus. The following discussion not only shows that $\mathcal{T}_r$ is connected but also shows how to visualize the torus. The basic idea is to describe $\mathcal{T}_r$ as some sort of bundle lying over $U_r=\pi(\mathcal{T}_r)\subseteq S^2$. The next argument shows that U_r is the closed region of S^2 which is shaded in Figure 5. Suppose $(x,v)\in\mathcal{T}_r$ and $x\neq n, s$. Then on T_xS^2, the inverse image $L^{-1}(l)$ is the affine line

$$l = x_2v_1-x_1v_2$$

with $x_1\neq 0$ or $x_2\neq 0$. The closest point of $L^{-1}(l)$ to the origin of T_xS^2 is the vector

$$v^0 = \frac{l}{x_1^2+x_2^2}(x_2,-x_1,0).$$

Since $\|v\|^2\geq\|v^0\|^2$ for all $v\in L^{-1}(l)\cap T_xS^2$, using $1=x_1^2+x_2^2+x_3^2$, we obtain

$$2(h-x_3) = 2(H(x,v)-x_3) \geq 2(H(x,v^0)-x_3)=\frac{l^2}{1-x_3^2} \qquad (*)$$

(see Figure 3). Thus U_r is the set of all $x\in S^2$ satisfying (*). Consider the cubic polynomial

$$V(x_3) = (1-x_3^2)(h-x_3)$$

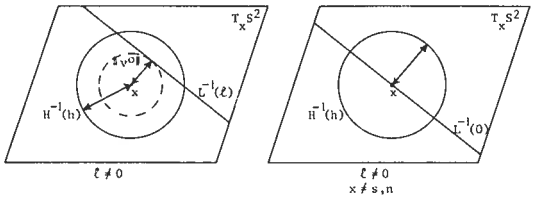

Figure 3.
Geometry of $H^{-1}(h)$ and $L^{-1}(l)$ in a fixed tangent space T_xS^2.

(see Figure 4). Then $V^{-1}([\frac{1}{2}l^2,\infty[)=[z_-,z_+]$ is the set of all $x_3\in[-1,1]$ which

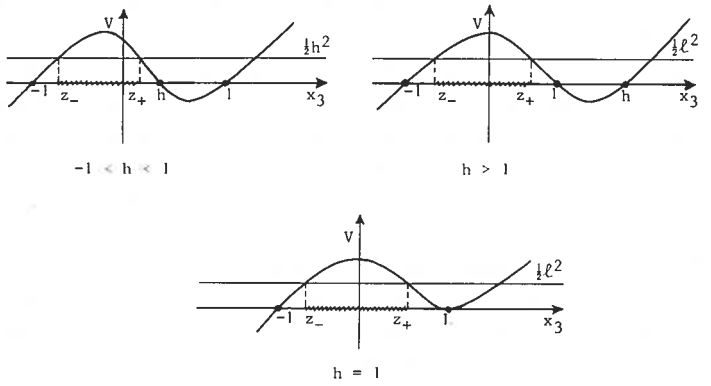

Figure 4.
Graph of V with $V^{-1}([\frac{1}{2}l^2,\infty[),\frac{1}{2}l^2<\max_{x\in[-1,1]}V(x)$ indicated by hatched interval $[z_-,z_+]$.

satisfy (*). As long as

$$0<\tfrac{1}{2}l^2<V_m=\max_{x_3\in[-1,1]}V(x_3)$$

the interval $[z_-,z_+]$ does not degenerate to a point and also is properly contained in $[-1,1]$. Thus U_r is the closed annular region of S^2 bounded by the two circles $C_n:x_3=z_+$ and $C_s:x_3=z_-$. When $l=0$ and $-1<h<1$, U_r is the closed region of S^2 containing the south pole s and bounded by $C_n:x_3=h$.

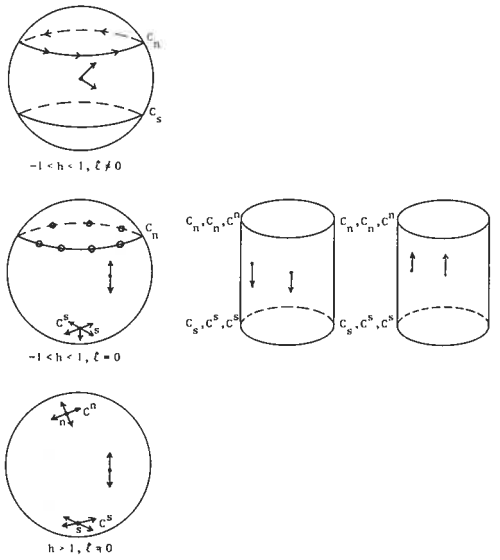

Figure 5.
Description of T_r as a bundle over U_r.

When $l=0$ and $h>1$, then $U_r=S^2$. To complete our picture of $\mathcal{T}_r$ as a

bundle over U_r we must determine the fiber $\pi^{-1}(x) \in \mathcal{T}_r$ over $x \in U_r$. A close look at Figure 3 shows that if $l \neq 0$ and equality holds in (*), that is, x lies on the boundary ∂U_r of U_r, then v must be equal to v^0. Thus the fiber of $\mathcal{T}_r$ over $x \in \partial U_r$ is a single vector v^0 with zero third component. If $l \neq 0$ and strict inequality holds in (*), that is, x lies in the interior of U_r, then the fiber $\pi^{-1}(x)$ of $\mathcal{T}_r$ consist of two vectors with nonzero third component. Now suppose $l = 0$ and $-1 < h < 1$. Then for $x \in \partial U_r$, that is, $x_3 = h$, $\pi^{-1}(x)$ is the zero vector. If $x \in U_r - \{s\}$, $\pi^{-1}(x)$ consists of two nonzero vectors of opposite sign. If $x = s$, then $\pi^{-1}(x)$ is the circle $C^s : \|v\|^2 = 2(h+1)$ in $T_s S^2$, since $L^{-1}(0) \cap T_s S^2 = T_s S^2$. Finally suppose that $l = 0$ and $h > 1$. Then for $x \in U_r - \{s, n\}$, $\pi^{-1}(x)$ is two nonzero vectors of opposite sign; while $\pi^{-1}(s)$ is the circle $C^s : \|v\|^2 = 2(h+1)$ in $T_s S^2$ and $\pi^{-1}(n)$ is the circle $C^n : \|v\|^2 = 2(h-1)$ in $T_n S^s$ (see Figure 5). This completes the description of $\mathcal{T}_r$ as a bundle over U_r. To see that $\mathcal{T}_r$ is a two dimensional torus, we first split each of the circles C_n, C_s or C^s, C^n into two disjoint circles. Over the remaining points of U_r the fibers of $\mathcal{T}_r$ consists of two vectors with nonzero third component. Taking those vectors with positive (negative) third component, we construct two cylinders, each with two labeled circles as boundary. Identifying the circles with the same label gives a two dimensional torus. (cf. Figure 6)

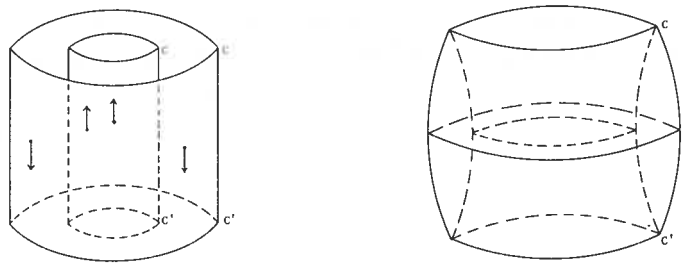

Figure 6.
Identification of regular fiber with a 2-torus

d. Critical fibers

Now we turn our attention to determining the topology of the fibers over the critical values. The fiber corresponding to the critical value $(-1,0)$ is the stable equilibrium $(s,0)$, that is, $\mathfrak{F}\mathfrak{M}^{-1}(-1,0) = (s,0)$. By construction the fiber corresponding to a relative equilibrium with critical value (l, h) is a circle in TS^2 corresponding to a positively (negatively) oriented horizontal circle in S^2 if $l > 0$ ($l < 0$) and its oriented tangent vector of length h. Only the topology of

$\mathcal{T}=\mathcal{EM}^{-1}(1,0)$ corresponding to the critical value of the unstable equilibrium needs to be found. Clearly $\pi(\mathcal{T})=S^2$. The fiber of $\mathcal{T}$ over $x\in S^2-\{s, n\}$ consists of two vectors of opposite sign with nonzero third component; the fiber over s is a circle C^s; and the fiber over n is the zero vector (see Figure 7).

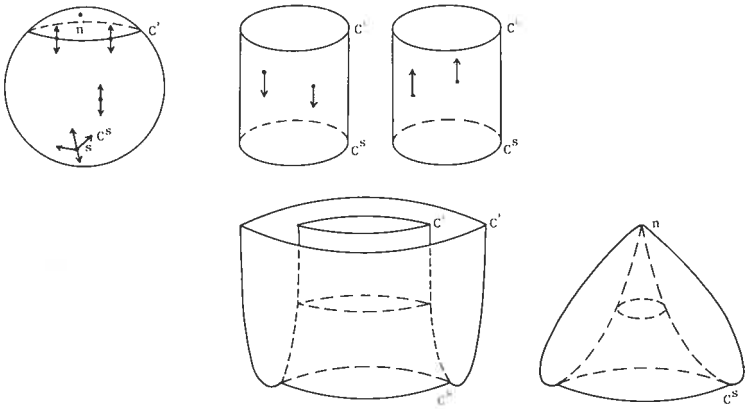

Figure 7.
Identification of singular fiber $E\mathbf{M}^{-1}(1,0)$ as one point compactification of a cylinder.

Cut off a small circle C^ϵ near n. Split C^ϵ and C^s into two circles and form two cylinders from the vectors in the fiber of $\mathcal{T}$: one from the vectors with positive third component and the other from the vectors with negative third component. Join the circles labeled C^s together and collapse both C^ϵ circles to a single point. Thus $\mathcal{T}$ is a one point compactification of cylinder. In other words, $\mathcal{T}$ is a 2-sphere with its north and south pole pinched to a point.

e. Energy surface

Next we determine the topology of each energy surface $H^{-1}(h)$, $h>-1$. Let $\tilde{\pi}=\pi|H^{-1}(h)$. Suppose $-1<h<1$. Then $H^{-1}(h)$ is smooth. Since $2(h-x_3)=\|v\|^2\geqslant 0$, $\pi(H^{-1}(h))=\{x\in S^2|x_3\leqslant h\}$ which is topologically a closed 2-disc $\overline{D}^2$. Over $x\in\overline{D}^2$ the fiber $\tilde{\pi}^{-1}(x)$ of $H^{-1}(h)$ is the circle $\{v\in T_xS^2|\|v\|^2=2(h-x_3)\}$; while over $x\in\partial\overline{D}^2$, $\tilde{\pi}^{-1}(x)$ is the zero vector. Split $\overline{D}^2$ along a diameter $\mathfrak{L}$ into two disjoint half open discs $D_\pm$ and let $\mathfrak{L}_u^\pm$, $u\in]-1,1[$, be a fibering of $D_\pm$ by parallel half open line segments perpendicular to $\mathfrak{L}$ (see Figure 8). For each $u\in]-1,1[$, the inverse image $\tilde{\pi}^{-1}(\mathfrak{L}_u^\pm)$ is topologically a 2-disc $\mathfrak{D}_u^2$, being the union of circles which shrink to a point.

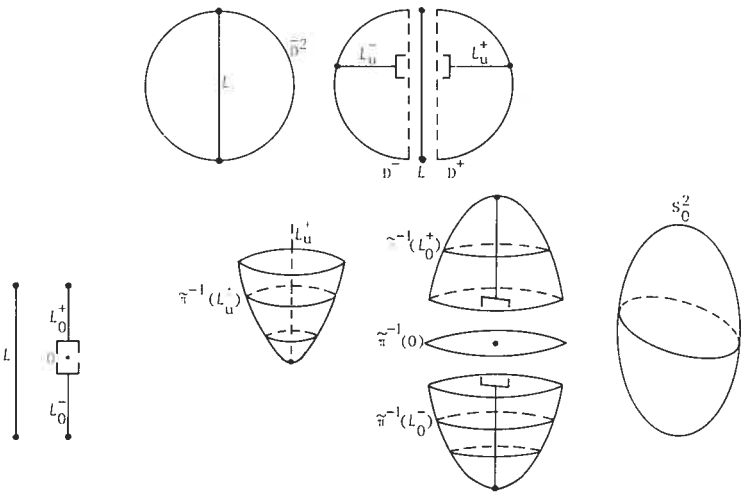

Figure 8.
Some of the building blocks of $H^{-1}(h)$, $-1<h<1$.

Therefore $\tilde{\pi}^{-1}(D_{\pm})$, being the union of 2-discs $\mathcal{D}_u$ over $u \in]-1,1[$, topologically a 3-disc $D^3_{\pm}$. As shown in the second row of Figure 8, $\tilde{\pi}^{-1}(\mathcal{L})$ is topologically a two sphere S^2_0. Therefore $H^{-1}(h)$ is the union of two 3-discs $D^3_{\pm}$ joined along a 2-sphere S^2_0. Hence, $H^{-1}(h)$ for $-1<h<1$ is topologically a three dimensional sphere S^3. Now suppose that $h>1$. Then $H^{-1}(h)$ is smooth and $\tilde{\pi}(H^{-1}(h))=S^2$. As before, over $x \in S^2$ the fiber $\tilde{\pi}^{-1}(x)$ is a circle in $T_x S^2$. Thus $H^{-1}(h)$ is topologically the tangent unit sphere bundle $T_1 S^2$ to S^2. But $T_1 S^2$ is the set of all pairs of orthonormal vectors in $\mathbb{R}^3$, which in turn is the set of all right handed orthonormal bases of $\mathbb{R}^3$. Therefore $H^{-1}(h)$ is the group $SO(3)$ of proper rotations of $\mathbb{R}^3$. Since $SO(3)$ is doubly covered by the special unitary group $SU(2)$, which is topologically a three dimensional sphere S^3, $SO(3)$ is topologically real projective three space $\mathbb{R}P^3$. When $h=1$, $H^{-1}(1)$ is not smooth, since it contains the critical point $(n,0)$. However $\tilde{\pi}(H^{-1}(1))=S^2$. Over $x \in S^2-\{n\}$, the fiber $\tilde{\pi}^{-1}(x)$ is a circle; while if $x=n$, $\tilde{\pi}^{-1}(n)=(n,0)$. Thus $H^{-1}(1)$ is $T_1 S^2$ with the fiber over n pinched to a point. All the information we have obtained about the topology of the fibers and energy level sets of the energy momentum map is summarized in Figure 9.

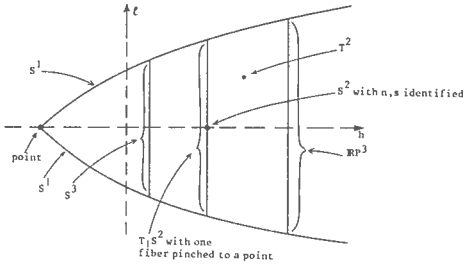

Figure 9.
Topology of fibers of energy momentum mapping.

f. Fitting together of fibers

We now show how the fibers of the energy momentum mapping fit together to form a fixed smooth energy surface. Fix $h \in]-1,1[\cup]1,\infty[$ and let $L_h^{\pm}$ be the intersection of the image of $\mathcal{EM}$ and a positive (negative) half line parallel with the l-axis. The fiber of $H^{-1}(h)$ over $L_h^{\pm}$ is a solid torus $ST^{\pm}$ which topologically is $S^1 \times D^2$. In view of the equation $H^{-1}(h) = \pi^{-1}(L_h^+) \cup \pi^{-1}(h,0) \cup \pi^{-1}(L_h^-)$, each smooth energy surface is the union of two solid tori $ST^{\pm}$ joined together along a two dimensional torus $T^2 = \pi^{-1}(h,0)$. More precisely, ST^+ and ST^- are glued together by an attaching mapping which is a diffeomorphism of T^2. The problem is: how to visualize this gluing mapping.

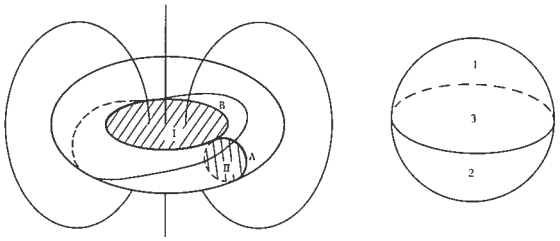

Figure 10.
S^3 as an S^1 bundle over S^2.

Suppose $-1<h<1$, then $H^{-1}(h)$ is S^3. The key observation is that S^3 is a fiber bundle over S^2 with fiber S^1 and group S^1 [7, p. 7]. Figure 10 gives a geometric realization of this bundle. Note that S^3 is thought of as the one point compactification of $\mathbb{R}^3$. Thus the vertical line in the figure is a circle. All the S^1 fibers pass transversally through either the 2-disc I or the 2-disc II, except the circles A and B which are the boundaries of I and II respectively. These 2-discs are identified with the hemispheres of S^2 with the same numbers; while the circles A and B are identified with the equator of S^2. The set of all fibers over each hemisphere of S^2 is a solid torus, being the union of all fibers which pass through either I or II; while the set of all fibers over the equator is T^2. Figure 11 shows the S^1 fibers on T^2 (oriented according to the action of the group S^1) from the point of view of the section "a" or "b" which corresponds to A or B respectively. All the S^1 fibers on T^2 can be throught of as the flow lines of a linear vectorfield on T^2. Taking the A circle as being horizontal, the flow lines are as depicted in the left hand side of Figure 11. The difference between the two left hand pictures is that in the first B is vertical while in the second the flow lines are vertical. This describes the "a" viewpoint. The "b" viewpoint is obtained similarly. The mapping ψ on T^2, given by $\begin{bmatrix} 1 & 0 \\ \pm 1 & 1 \end{bmatrix}$, is the change from the "a" viewpoint on T^2 to the "b"

viewpoint. Moreover, ψ shows how the solid torus ST^+ over

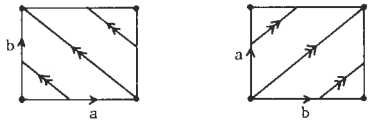

diagonal lines are S^1 fibers with arrows giving direction of S^1 action on fiber; dots joined by light lines give lattice defining T^2

S^1 fibers are vertical and viewpoint section horizontal; ψ maps a to a and b to b and is $\begin{bmatrix} 1 & 0 \\ -1 & 1 \end{bmatrix}$ with respect to standard basis.

Figure 11.
The gluing map for the solid torus decomposition of S^3.

the upper hemisphere is glued to the solid torus over the lower hemisphere. Given an orientation of T^2, the choice of sign in ψ is determined by the action of S^1 on the fibers [7, p. 135].

Suppose $h>1$, then $H^{-1}(h)$ is $\mathbb{R}\,\mathrm{P}^3$. Since every proper rotation of $\mathbb{R}^3$ is uniquely specified by giving an oriented axis of rotation and a right handed twist less than or equal to a half turn about this axis, $\mathbb{R}\,\mathrm{P}^3 = SO(3)$ can be visualized as a closed 3-disc $\overline{D}^3$ in $\mathbb{R}^3$ of radius ½. (The length of the oriented axis, which is a vector in $\mathbb{R}^3$, gives the fraction of a turn about the axis). On the boundary $\partial\overline{D}^3$, which is a two dimensional sphere, diametrically opposite points are identified. Figure 12 gives the geometric realization of $\mathbb{R}\,\mathrm{P}^3$ as an S^1 bundle over S^2. Again there are two 2-discs: I and II where II is the union of II' and II'' with diametrically opposite points on the heavy dashed line identified (see Figure 12).

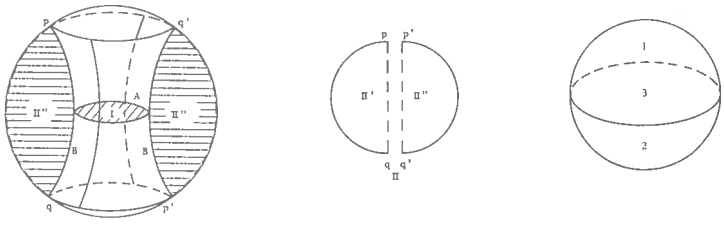

Figure 12.
$\mathbb{R}\,\mathrm{P}^3$ as an S^1 bundle over S^2.

All the S^1 fibers except A and B, pass transversally through either I or II. The S^2 is assembled as in the S^3 case and also the solid torus decomposition. The S^1 fibers on T^2 are again drawn from the *"a"* and *"b"* section viewpoints (see Figure 13). Note that the fiber B wraps twice around the hole of T^2 while wrapping once around the meridian. The mapping $\tilde{\psi}$ from the *"a"* to the *"b"* viewpoint is $\begin{bmatrix} 1 & 0 \\ \pm 2 & 1 \end{bmatrix}$, which is the gluing map of the solid tori in $\mathbb{R}\,\mathrm{P}^3$.

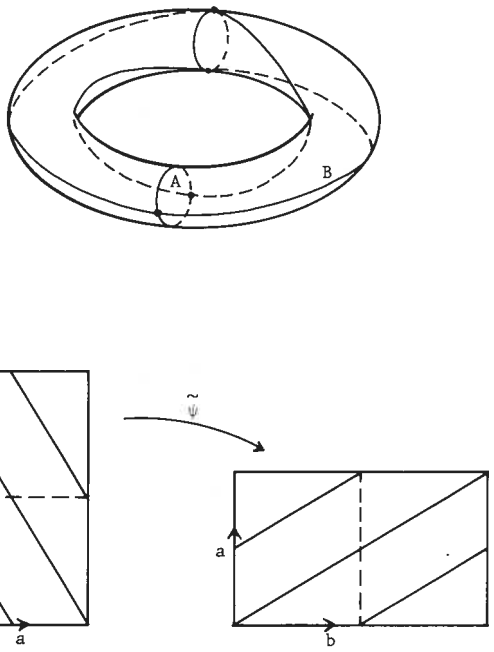

Figure 13.
The gluing map on T^2 for the solid torus decomposition of $R\,\mathrm{P}^3$.

2. Bifurcation and monodromy

a. Existence of monodromy.

A glance at Figure 9 discloses that as h passes through 1 the topology of the energy surface $H^{-1}(h)$ changes from that of a three dimensional sphere to

that of real projective three space. This bifurcation of $H^{-1}(h)$ (see Figure 14) is not due to a local bifurcation in the topology of the fibers of the energy momentum mapping, because over any open set U of regular values which does not contain (1,0), $\mathcal{EM}^{-1}(U)=U\times T^2$, that is, $\mathcal{EM}$ has two dimensional tori as fibers over U. In fact, the bifurcation of the energy surfaces signals the presence of monodromy in the energy momentum mapping, as the following discussion shows.

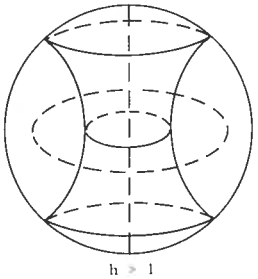

Antipodal points on S^2 identified

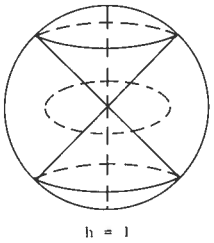

Antipodal points on S^2 identified.
Origin has conelike singularity.

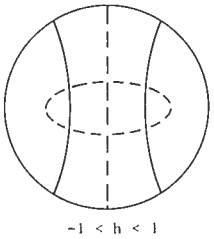

Figure 14.

S^2 identified to a point.
(Gives double cover of $h>1$ picture).

Let γ be a circle in the set $\mathcal{R}$ of regular values of $\mathcal{EM}$ with center at (1,0). Consider the bundle $\mathcal{B}=\mathcal{EM}^{-1}(\gamma)$ over γ with fiber T^2. Up to isomorphism $\mathcal{B}$ depends only on the homotopy class of γ in $\mathcal{R}$. Let $\Gamma^{\pm}$ be paths in the image of $\mathcal{EM}$ as drawn in Figure 15. Suppose that $\mathcal{B}$ is a trivial bundle, that is, $\mathcal{B}$ is diffeomorphic to $\gamma\times T^2$. Then $\mathcal{EM}^{-1}(\Gamma^-)$ is homeomorphic to $\mathcal{EM}^{-1}(\Gamma^+)$. But $\mathcal{EM}^{-1}(\Gamma^-)$ is homeomorphic to $H^{-1}(h')$ for some $h'\in]-1,1[$, which in turn is homeomorphic to S^3; while $\mathcal{EM}^{-1}(\Gamma^+)$ is homeomorphic to $H^{-1}(h'')$ for some $h''>1$ which in turn is homeomorphic to $\mathbb{R}\,\mathrm{P}^3$.

But S^3 and $\mathcal{R}\mathrm{P}^3$ are not topologically equivalent. Hence $\mathcal{B}$ is not a trivial bundle. Let $c\in\gamma$, then $\mathcal{B}'=\mathcal{EM}^{-1}(\gamma-\{c\})$ is a trivial T^2 bundle, since $\gamma-\{c\}$ is contractible. Therefore $\mathcal{B}$ is obtained from $\mathcal{B}'$ by a gluing diffeomorphism ϕ of $T^2=\mathcal{EM}^{-1}(c)$ into itself. The mapping ϕ is called the monodromy mapping of the bundle $\mathcal{B}$. Since isotopic monodromy mappings give rise to isomorphic bundles over γ, the fact that $\mathcal{B}$ is nontrivial implies that ϕ is not isotopic to the identity.

b. Calculation of monodromy.

A technical argument which is given below shows that the gluing maps of the S^1 bundles $\mathcal{EM}^{-1}(\Gamma^+)$ and $\mathcal{EM}(\Gamma^-)$ are respectively $\tilde{\psi}^- = \begin{bmatrix} 1 & 0 \\ -2 & 1 \end{bmatrix}$ and $\psi^- = \begin{bmatrix} 1 & 0 \\ -1 & 1 \end{bmatrix}$. Therefore the monodromy is $\phi = (\tilde{\psi}^-)^{-1} \circ \psi^- = \begin{bmatrix} 1 & 0 \\ 1 & 1 \end{bmatrix}$. We now give the technical argument. The nonexpert reader is advised to skip the remainder of the subsection.

In order to compute the monodromy of $\mathcal{B}$ we introduce a certain Ehresmann connection [8] on $\mathcal{B}$ which allows us to parallel transport geometric objects from one fiber of $\mathcal{B}$ to another. Using a partition of unity it suffices to construct the connection locally. A nice local trivialization of $\mathcal{B}$ over γ is given by a choice of action angle coordinates [1]. For each (h, l) in some connected open subset V of γ the construction of action angle coordinates gives a Hamiltonian vectorfield X_F on the fiber $T^2_{h,l}$ of $\mathcal{B}$ over (h,l) such that

1) X_F is a linear combination of the Hamiltonian vectorfields X_L and X_H associated with the Hamiltonian functions L and H respectively;
2) X_F on $T^2_{h,l}$ has only periodic orbits of period one;
3) X_L and X_F generate a lattice $L_{h,l}$ which defines $T^2_{h,l}$ and depends smoothly on $(h,l) \in V$.

Thus $\mathcal{B}_V$, the piece of $\mathcal{B}$ over V, is diffeomorphic to $V \times T^2$. On $\mathcal{B}_V$ we define the vertical vectorfields of our Ehresmann connection to be vectorfields which are linear combinations of X_L and X_F while the horizontal vectorfields are nonzero vectorfields on V. Using this connection, parallel translation ϕ^- along the piece Γ^- of γ which joins P to Q transports the lattice L_P into the lattice L_Q (see Figure 15). Thus ϕ^- is a diffeomorphism of T^2_P onto T^2_Q which is the gluing map $\begin{bmatrix} 1 & 0 \\ \pm 1 & 1 \end{bmatrix}$ of the bundle $\mathcal{EM}^{-1}(\Gamma^-)$. Similarly, parallel translation ϕ^+ along the piece Γ^+ of γ joining P to Q is the gluing map $\begin{bmatrix} 1 & 0 \\ \pm 2 & 1 \end{bmatrix}$ of the bundle $\mathcal{EM}^{-1}(\Gamma^+)$.

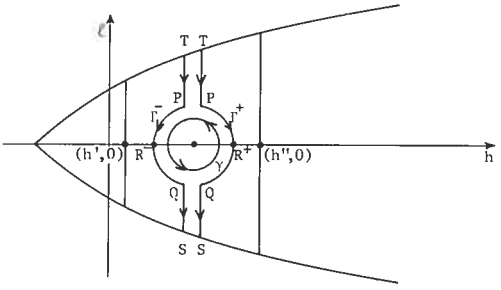

Figure 15.
Monodromy and bifurcation of the energy surfaces.

We now have to answer the delicate question of which sign to choose in ϕ^- and ϕ^+. As remarked earlier the sign choice is determined by the orientation

of the bundle space (which induces an orientation on the two dimensional torus T^2) and the orientation induced by the action of the group S^1 on the oriented fiber S^1. In our case we determine the sign as follows. Let $p \in \Gamma^{\pm}$ and $\hat{p} \in T_p^2$. Suppose that $X_H(\hat{p})$ and $X_F(\hat{p})$ are linearly independent at $\hat{p}$. (This does not depend on the choice of $\hat{p} \in T_p^2$). We say that the Hamiltonian vectorfield X_H on T_p^2 has positive sense with respect to the ordered basis $\{X_L(\hat{p}), X_F(\hat{p})\}$ of the lattice L_p, if $X_H(\hat{p}) = \alpha X_L(\hat{p}) + \beta X_F(\hat{p})$ where either $\alpha > 0$ and $\beta > 0$ or $\alpha < 0$ and $\beta < 0$; otherwise X_H has negative sense. When parallel transporting L_p along $\Gamma^{\pm}$ from P to Q, X_H and X_F are linear dependent only at $R^{\pm}$ (see Figure 15) that is, when $l = 0$, because only then does X_H have a periodic flow on $T^2_{h,0}$. As l changes sign, X_L does also; more precisely, $X_L(p') = -X_L(\hat{p})$ where $p = (h,l) \in \Gamma^{\pm}$, $l > 0$ and $p' = (h,-l) \in \Gamma^{\pm}$. Since X_H and X_F are continuous, when l changes sign, the sense of X_H changes as p passes through $R^{\pm}$. Since the only sense change occurs at $R^{\pm}$ and by a suitable choice of X_F the sense of X_H at P can be made positive, the sense of X_H at Q, after being transported along Γ^- (Γ^+) from P to Q, is negative. Therefore the signs of both attaching maps $\phi^{\pm}$ are negative. Hence parallel translation along Γ^- from P to Q followed by parallel translation along the inverse of Γ^+ from Q to P defines a diffeomorphism ϕ of T_P^2 into itself which is given by

$$\phi = (\phi^+)^{-1} \circ \phi^- = \begin{bmatrix} 1 & 0 \\ -2 & 1 \end{bmatrix}^{-1} \begin{bmatrix} 1 & 0 \\ -1 & 1 \end{bmatrix} = \begin{bmatrix} 1 & 0 \\ 1 & 1 \end{bmatrix}.$$

ϕ is the monodromy mapping of the bundle $\mathcal{EM}^{-1}(\gamma)$ where $\gamma = (\Gamma^+)^{-1} \circ \Gamma^-$.

c. Other calculations of monodromy.

In addition to the above calculation, there are three other entirely different arguments which compute the monodromy of the spherical pendulum. The first is a physical geometric argument of Duistermaat [1] which will not be repeated here. The second one due to F. Ehlers in Bonn in essence shows that $\mathcal{EM}$ for values close to (1,0) is isomonodromic with its 2-jet at $(n,0)$. This result is nontrivial because $(n,0)$ is not a finitely determined singularity of $\mathcal{EM}$. On the other hand, the 2-jet of $\mathcal{EM}$ at $(n,0)$ is the energy momentum mapping of the two dimensional harmonic oscillator, for which the monodromy is easy to compute. For further details see [9]. In this same paper Min Oo in Bonn gives the following sequence of pictures (Figure 16) which geometrically computes the map $\phi_* : H_1(T_p^2) \to H_1(T_p^2)$ on homology induced by the monodromy ϕ. (Notice that the conventions in Figure 16 are the same as those in Figure 5). Here it is sketched how the two generators δ_0, ϵ_0 of the homology group are transformed when moved around the isolated singular value on γ.

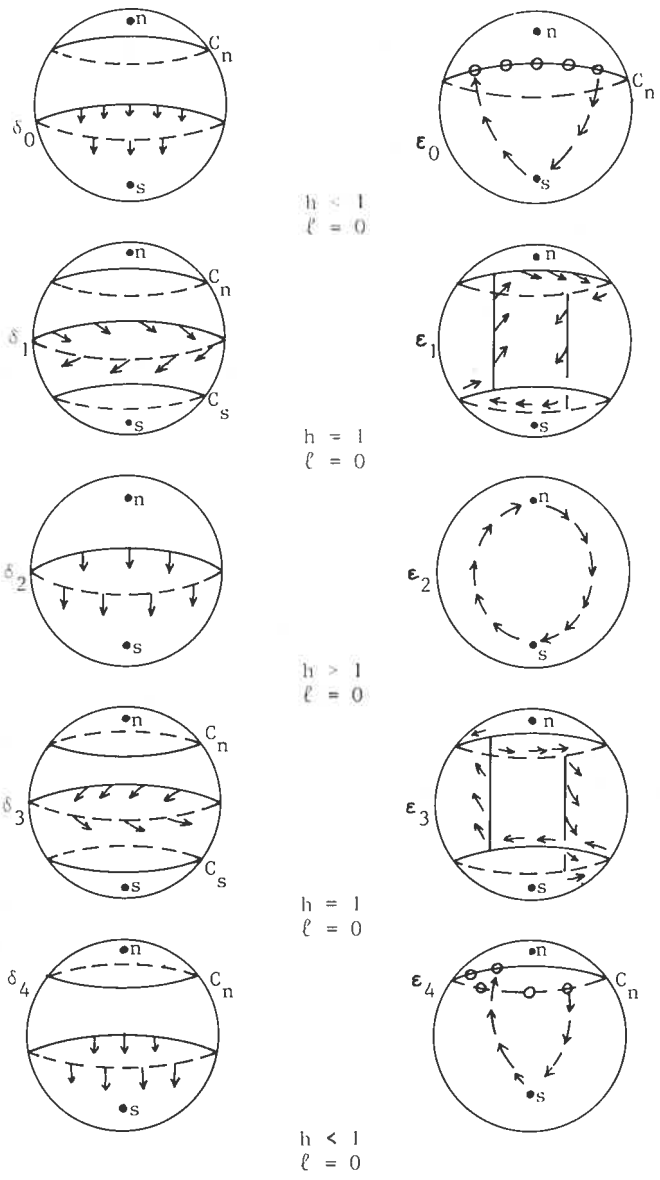

Figure 16.
Monodromy on Homology.
For $l=1,2,3,4$ cycles δ_l, ϵ_l are basis of homology of $T^2_{k,l}$ obtained by homotopy from $\delta_{l-1}, \epsilon_{l-1}$, $l=1,2,3,4$. ϵ_4 is homologous to $\epsilon_0+\delta_0$ and δ_4 and δ_0. Thus $\psi_r = \begin{bmatrix} 1 & 0 \\ 1 & 1 \end{bmatrix}$ on homology.

3. Acknowledgements

To the expert reader my debt to Prof. J.J. Duistermaat in Utrecht is obvious. Also I would like to thank Drs. Min Oo and F. Ehlers for showing me their alternative methods for calculating the monodromy. Finally the geometric visualization of the gluing maps given in Figures 9-12 is due to Dr. Tim Poston of UCLA.

4. References

[1] J.J. Duistermaat, *On global action-angle coordinates,* Comm. Pure Appl. Math., **33** (1980), 687-706.

[2] H. Goldstein, *Classical mechanics,* 1st ed., Addison-Wesley, Reading, Mass., 1959.

[3] V.I. Arnold, *Mathematical methods of classical mechanics,* Springer Verlag, New York, 1978.

[4] S. Smale, *Topology and mechanics I,* Invent. Math., **10** (1970), 305-331.

[5] K. Symon, *Mechanics,* Addison-Wesley, Reading, Mass, 1961.

[6] A.G. Webster, *The dynamics of particles and rigid, elastic, and fluid bodies,* 2nd ed., Dover, 1959.

[7] N. Steenrod, *Topology of fiber bundles,* Princeton Univ. Press, Princeton, 1951.

[8] J. Wolf, *Differentiable fibre spaces and mappings compatible with Riemann metrics, Mich. Math. J.,* **11** (1964), 65-70.

[9] R. Cushman, F. Ehlers, and Min Oo, *Three proofs of monodromy in the spherical pendulum* (in preparation).

Author's address:
Mathematics Institute
Rijksuniversiteit Utrecht
Budapestlaan 6
3508 TA Utrecht
The Netherlands